J. Earth Syst. Sci. (2019) 128:119
https://doi.org/10.1007/s12040-019-1156-z
© Indian Academy of Sciences

The influence of local meteorology and convection on carbon monoxide distribution over Chennai

L K Sahu[1,*], Nidhi Tripathi[1,2], Varun Sheel[1] and N Ojha[1]

[1] *Physical Research Laboratory (PRL), Navrangpura, Ahmedabad 380 009, India.*
[2] *Indian Institute of Technology Gandhinagar, Palaj, Gandhinagar 382 355, India.*
**Corresponding author. e-mail: lokesh@prl.res.in, l_okesh@yahoo.com*

MS received 11 July 2018; revised 14 November 2018; accepted 27 December 2018; published online 8 May 2019

The influence of local meteorology and convection activities on the vertical distribution of carbon monoxide (CO) over Chennai in southern India was investigated by analysing the measurements of ozone aboard airbus in-service aircraft observations during the years 2012–2013. The seasonal variation of CO in the free troposphere was observed to be different and less pronounced than that in the planetary boundary layer (PBL). The near surface mixing ratio of CO was the highest (190 ± 68 ppbv) during winter, while enhanced values (117 ± 11 ppbv) in the free troposphere were observed during post-monsoon. The mixing ratios were the lowest throughout the troposphere during the monsoon. In the PBL, the mixing ratios of CO showed a decline with an increase in wind speed and were the highest (>200 ppbv) under stagnant conditions ($1-2$ m s^{-1}) during winter. The higher CO in the lower free troposphere during the pre-monsoon period is attributed to the stronger biomass burning emissions. In the middle–upper troposphere, higher levels of CO during post-monsoon are due to the enhanced vertical mixing of regional emissions associated with weaker wind shears and frequent convection activities. Overall, the contrasting effects of stronger CO emissions can be observed in winter/pre-monsoon, while the efficient vertical mixing during the monsoon/post-monsoon season governs the observed seasonality of CO. The model for ozone and related chemical tracers, version 4 (MOZART-4) provides a reasonable representation of the convection effect on the CO mixing ratio. This study highlights a need to conduct more observations, especially of aircraft-borne instruments, to understand the effects of regional-scale emissions and dynamics in the middle–upper tropospheric chemistry over South Asia.

Keywords. Carbon monoxide; convection; India; simulation; troposphere; biomass burning.

1. Introduction

Carbon monoxide (CO) is produced by the incomplete combustion of various carbon fuels of both biomass and fossil origins. The mixing ratio of CO is widely used as a tracer of polluted air in remote regions mainly due to its specific emission sources and longer atmospheric lifetimes of about 2 months (Stohl *et al.* 2002). The major sources of CO emissions are biomass burning and anthropogenic activities including the usage of fossil fuels (e.g., Shindell *et al.* 2006; Jöckel *et al.* 2016). Yoon and Pozzer (2014) estimated a rapid increase in CO mixing ratios over South Asia due to the increasing anthropogenic emissions by combining observations with a global climate model. In urban and polluted regions, the oxidation of CO can lead to the formation of ozone (O_3) in the presence of oxides of nitrogen ($NOx = NO + NO_2$) and sunlight (Fishman and Seiler 1983).

Additionally, CO is a criterion pollutant as exposure to its elevated levels adversely affects the regional to global air quality and human health (Prockop and Chichkova 2007; Anenberg *et al.* 2009). Therefore, it is important to investigate the spatio-temporal variations of CO and the contribution of various emission sources, especially over the South Asia region where anthropogenic activities are increasing rapidly and the studies are limited.

The mixing ratios of CO in the troposphere are influenced by a variety of both emission and atmospheric processes. The updraft of lower tropospheric air, mostly through convection, tends to increase CO in the middle and upper troposphere (e.g., Rauthe-Schöch *et al.* 2016). The deep convection in the South Asia region is identified as a key mechanism for the transport of pollution from the troposphere to the lower stratosphere (Randel *et al.* 2010; Lelieveld *et al.* 2018 and references therein). During the past 2–3 decades, anthropogenic emissions of CO have been increasing at a rate of around 2.3% yr^{-1} (Ohara *et al.* 2007); however, the in situ observations of CO profiles in this region remain very limited. Most of the previous studies of the vertical distribution of CO over the Indian region have relied on the satellite observations (e.g., Kar *et al.* 2008; Ghude *et al.* 2011; Girach and Nair 2014). In recent years, measurements of CO from the space-based instruments such as the measurement of pollution in the troposphere (MOPITT) retrievals are used to study the global distribution of CO (Worden *et al.* 2013 and references therein). However, satellite retrievals have limited validation in this region and significant differences have been reported in CO profiles among satellite retrievals, in situ observations and model results, especially under cloudy and rainy conditions (Ojha *et al.* 2016).

In this study, we analyse the vertical profiles of CO measured during the measurements of ozone aboard airbus in-service aircraft (MOZAIC) flights over Chennai airport (12.98°N and 80.16°E) in southern India. Sahu *et al.* (2018) reported a detailed study of seasonal variations of CO and the impact of biomass burning and long-range transport over Chennai. The primary objective of this paper is to investigate the impact of local meteorology and convection activities in the southern part of India. However, briefly, in the context of the tropospheric response to convection, a comparison between the measurement and the model for ozone and related chemical tracers (MOZART-4) simulation of CO mixing ratio is also presented.

2. Study region and data set

The MOZAIC project was initiated by the scientists, aircraft manufacturers and airliners from Europe in the year 1993 with an objective to study the variability of the trace gases of the atmosphere. The measurements taken during both take-off and landing of the flight provide the vertical profile data. The MOZAIC measurement data of the CO mixing ratio is available from the in-service aircraft for a global observing system (IAGOS) (http://www.iagos.org). The in situ detection of CO using absorption at 4.67 μm was performed using a gas filter correlation-based technique (Model 48CTL, Thermo Environmental Instruments). A precision of ±5 ppbv, calibration uncertainty of ±5% and a limit of detection (LoD) of 10 ppbv were estimated for a time response of 30 s (Nedelec *et al.* 2003). A total of 129 vertical profiles of CO and meteorological parameters were measured over Chennai airport during the March 2012–June 2013 period. The response time of the CO analyser is 4 s which translates into a vertical resolution of 30 m altitude; however, 150-m vertical resolution data are recommended for scientific use. The MOZART-4 version includes 85 gaseous species, 12 bulk aerosols, 39 photolysis and 157 reactions in the gas phase (Emmons *et al.* 2010). The input meteorological fields were obtained from the National Center for Environmental Prediction–Global Forecast System (NCEP–GFS). The precursors of ozone and their effects in the troposphere (POET) inventory data were taken for the emissions from anthropogenic sources (Granier *et al.* 2005). The gridded (1° × 1°) POET inventory included the anthropogenic, open fire and natural emissions. MOZART-4 simulations have been conducted in three Teraflops (TFLOPS) high-performance computing clusters with 20 nodes at the Physical Research Laboratory (PRL) (Sheel *et al.* 2014).

According to census 2011, Chennai city had a population of 4.68 million and the urban agglomeration had a population of 8.65 million. In the last decade (2001–2011), the city registered a population growth of about 7.7% yr^{-1} (https://smartnet.niua.org). According to an estimate for the year 2012, the total vehicle population of Chennai was about 3.76 million (http://www.tn.gov.in/sta/eng%20cc/REG.html). It is the biggest industrial and commercial centre in south India. Most of the industrial estates such as Manali, Ennore, Ambattur, Thiruvottriyur, etc., are located on the northern outskirts of the city. The seasonal wind in South Asia is controlled by the location of the intertropical convergence zone (Asnani 2005). The post-monsoon season, also known as the north-east (NE) monsoon, is the principal rainy period in Tamil Nadu and some other parts of peninsular India. The rainfall from the NE monsoon accounts for about 60% of the yearly rainfall in the coastal regions of Tamil Nadu state (http://imdpune.gov.in/Weather/Forecasting_Mannuals/IMD_IV-18.4.pdf). On the other hand, unlike the northern parts of India, the SW monsoon is the secondary rainy period. The SW monsoon circulation is characterised by a large-scale convergence near the surface coupled with a strong divergence in the upper troposphere. The four seasons in India are defined as the winter (December–February), pre-monsoon (March–May), monsoon (June–September) and post-monsoon (October–November) months.

Outgoing longwave radiation (OLR) provides information on regional meteorological variations (Ueno and Aryal 2007) and the cloud convection is a primary mechanism which controls the distribution of OLR over the tropics. The development of deep convection over the South Asia region is inhibited by the El Niño conditions while favoured by the La Niña conditions, resulting in the higher and lower values of OLR, respectively (Girishkumar and Ravichandran 2012). In this study, the daily OLR data obtained from the NOAA's Climate Diagnostics Center (CDC) have been used to investigate the role of the prevailing El Niño-Southern Oscillation (ENSO) conditions in the trend of upper tropospheric CO. Particularly, in the context of transitioning from a mild El Niño 2012 to a weak La Niña 2013, back trajectory analysis, multivariate ENSO index (MEI, https://www.esrl.noaa.gov/psd/enso/mei/), moderate resolution imaging spectro radiometer (MODIS) fire count (http://modis-fire.umd.edu/index.php), etc., are used to investigate the role of convection, biomass burning and ENSO.

3. Results and discussion

3.1 *Seasonal variation of vertical CO*

The profiles of CO mixing ratio and wind speed measured during different seasons are shown in figure 1. The seasonal mean (± standard deviation) mixing ratios of CO (ppbv) measured at different altitudes of 0–2, 2–4, 4–6, 6–8, 8–10 and 10–12 km over Chennai are presented in table 1. The profiles of both CO and wind speed show strong seasonal and vertical variations. Near surface (0–2 km) CO mixing ratios over Chennai are observed to be higher during the winter (190 ± 68 ppbv) and post-monsoon (185 ± 52 ppbv) seasons, whereas the lowest levels are observed during the summer monsoon (124 ± 33). In the lower mid-troposphere (2–6 km), the mixing ratios of CO show a different seasonal dependence with high values in the pre-monsoon and the lowest in the monsoon season. At greater heights (6–12 km), the average mixing ratios of CO were decreased in the order of the post-monsoon (117 ± 11 ppbv), winter (102 ± 5 ppbv), pre-monsoon (97 ± 5 ppbv) and monsoon (82 ± 6 ppbv) seasons, respectively. Clearly, the mixing ratios of CO in the monsoon season were lower than the values observed in other seasons throughout the troposphere. It is also important to note that the seasonal variation of the CO mixing ratio in the troposphere shows different patterns depending on altitude. Overall, the seasonal variation of CO in the free troposphere (4–12 km of altitudes) is less pronounced than in the planetary boundary layer (PBL). The seasonal mean values of wind speed (m s^{-1}) measured at different altitudes over Chennai are also shown in figure 1. The average wind speed values measured between 0 and 2 km of altitudes were $11 \pm 6, 10 \pm 6, 19 \pm 9$ and 14 ± 8 ppbv in the winter, pre-monsoon, monsoon and post-monsoon seasons, respectively. From the surface up to 6 km, the values of wind speed measured in the monsoon and post-monsoon seasons were higher than those measured during the winter and pre-monsoon seasons. Meanwhile, between 6 and 12 km of altitudes, the values of wind speed measured in the post-monsoon season were lower than the values observed in other seasons. Overall, the seasonal variation of wind speed in the free troposphere was more pronounced than in the lower troposphere. CO mixing ratios generally showed a contrasting seasonality to that of the wind speed throughout the troposphere. Consistent with the observations, the model also shows stronger seasonal variations in the lower troposphere than in the free troposphere. In the lower troposphere, the MOZART-4 simulates the lowest value of 92 ± 19 ppbv for the month of July and the highest value of 158 ± 30 ppbv for the month of November. In the middle and upper troposphere, the MOZART-4 simulates the lowest value of 83 ± 5 ppbv for the month of July and the highest value of 123 ± 6 ppbv for the October–November

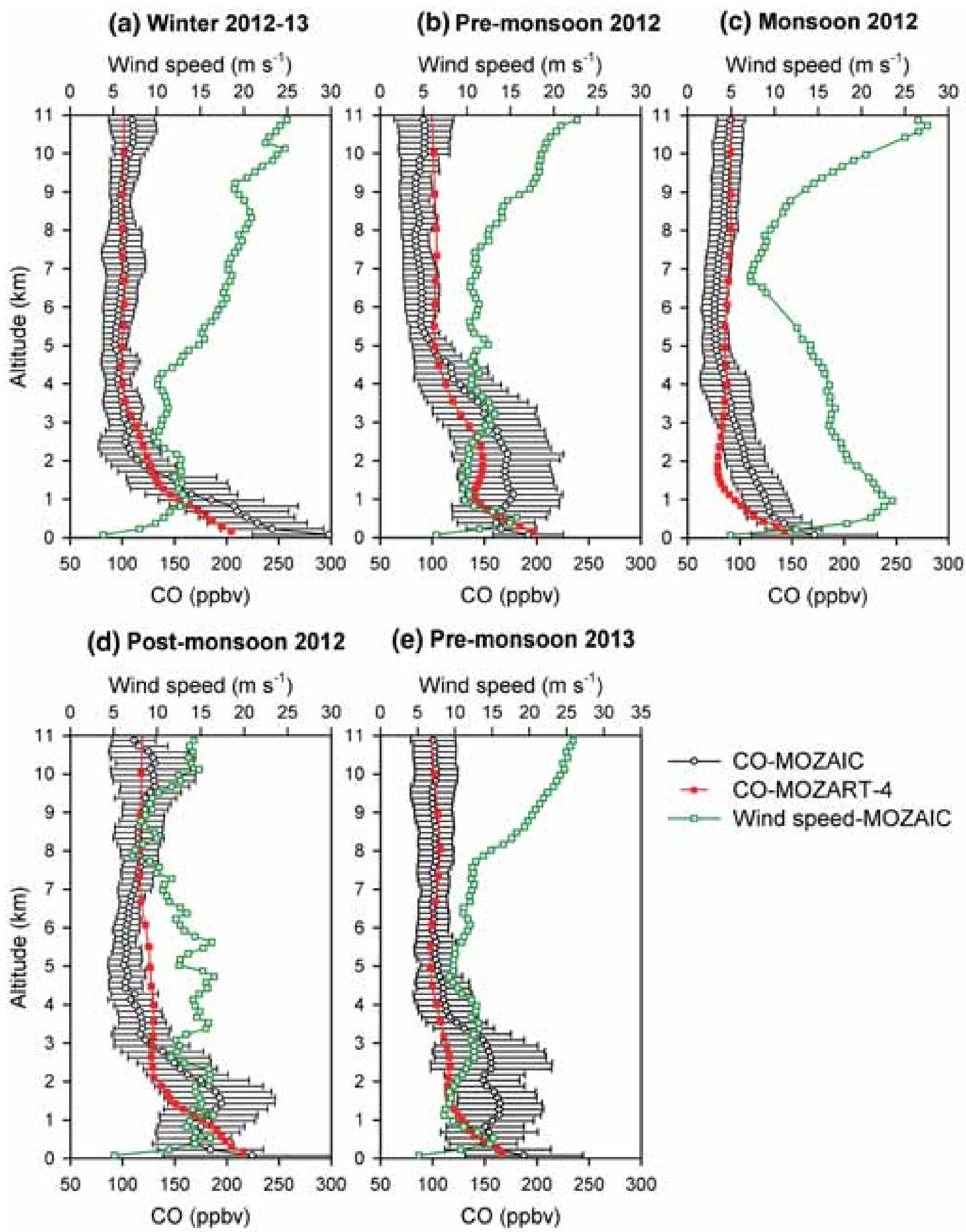

Figure 1. Vertical profiles of the CO mixing ratio and wind speed measured during different seasons over Chennai. MOZART-4 simulated vertical profile of CO is also shown for comparison.

Table 1. *Mean (± standard deviation) of CO and wind speed measured at 0–2, 2–4, 4–6, 6-8, 8–10 and 10–12 km of altitude over Chennai in the winter, pre-monsoon, monsoon and post-monsoon seasons.*

	Winter		Pre-monsoon		Monsoon		Post-monsoon	
Altitude (km)	CO (ppbv)	Wind speed ($m\ s^{-1}$)	CO (ppbv)	Wind speed ($m\ s^{-1}$)	CO (ppbv)	Wind speed ($m\ s^{-1}$)	CO (ppbv)	Wind speed ($m\ s^{-1}$)
0–2	190 ± 68	11 ± 6	166 ± 44	11 ± 6	124 ± 33	19 ± 9	185 ± 52	14 ± 8
2–4	103 ± 21	11 ± 6	148 ± 47	12 ± 5	92 ± 20	17 ± 7	129 ± 33	14 ± 9
4–6	96 ± 14	14 ± 8	104 ± 24	11 ± 6	77 ± 15	13 ± 8	101 ± 14	15 ± 10
6–8	101 ± 17	19 ± 9	94 ± 16	12 ± 7	78 ± 12	8 ± 5	110 ± 17	11 ± 6
8–10	101 ± 12	21 ± 13	94 ± 19	18 ± 11	85 ± 13	14 ± 8	123 ± 28	10 ± 7
10–12	109 ± 20	24 ± 13	97 ± 23	23 ± 14	90 ± 13	27 ± 13	121 ± 28	14 ± 13

period. The MOZART-4 profile in the lower region exhibits a higher disagreement with the MOZAIC measurements for the monsoon season.

The spatio-temporal variability of CO in the troposphere depends on the source locations and the mixing/transport associated with the horizontal and vertical winds (Sheel *et al.* 2016). In the lower troposphere, the strength of local emission, dilution due to horizontal winds and vertical ventilation due to convection control the seasonal variations of primary pollutants such as CO. In contrast, the seasonality of CO aloft strongly depends on the vertical transport near the ground to the middle and upper troposphere, especially in the tropics favoured by strong convection activities (Sheel *et al.* 2014). The lowest values of the CO mixing ratio and wind speed were observed in mid-tropospheric altitudes throughout the year. Weaker or negative wind shears allow the efficient vertical transport of the near-surface air masses. When the wind shear is weak, the convection grows at a greater height and facilitates a rapid vertical mixing of the troposphere. Therefore, weaker wind shears in the post-monsoon season are expected to cause the rapid transport of CO-rich surface air to the free troposphere. In other words, enhancements of the CO mixing ratio in the free troposphere during the post-monsoon period are mostly due to an increase in convection activities. This is consistent with the microwave limb sounder (MLS) data which show widespread enhancements of CO in the upper troposphere over South Asia during the monsoon and early post-monsoon seasons (Zhang *et al.* 2011). Sahu *et al.* (2018) have reported a detailed study of CO variation using the MOZAIC and MOZART-4 data with an emphasis on the impact of tropical cyclones over the Bay of Bengal (BOB).

In addition to local meteorological factors, the seasonal changes in the long-range transport and biomass burning play an important role in the seasonal variation of CO. The back trajectory analysis provides information on the source and long-range transport of air masses. However, to assess the impact of transport on the vertical distribution of CO, the 7-day back trajectories (6 h, $1.25° \times 1.25°$) over Chennai at 1 km of height were calculated using the JRA-25 and JMA Climate Data Assimilation System (JCDAS). The seasonal back trajectories are overlaid onto the fire count maps (see figure 2). Except for the monsoon season,

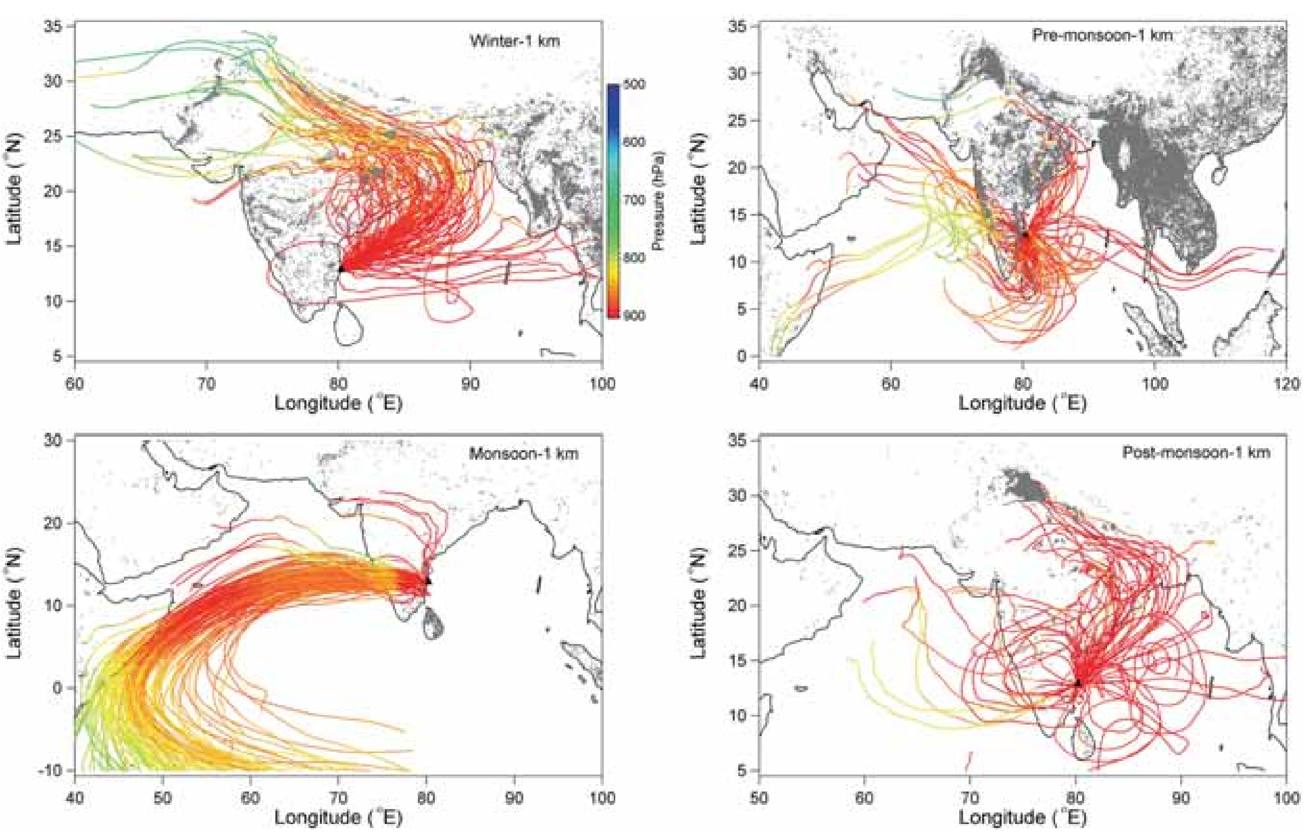

Figure 2. Back trajectories at 1 km of altitude over Chennai during different seasons and the grey dots represent the MODIS fire counts.

trajectories at 1 km of altitude suggest the flow of pollutants from the Indo-Gangetic Plain, whereas trajectories for the monsoon season suggest that the transport of cleaner air originates over the Arabian Sea and the western Indian Ocean.

3.2 *Impact of local wind*

Besides the local emissions, the spatio-temporal distribution of CO in the lower troposphere is influenced by the local- and synoptic-scale meteorology (Sahu *et al.* 2011, 2018; Yadav *et al.* 2014). Influences of meteorological parameters on gaseous and particulate pollutants have been reported for several urban sites in the South and South East Asia regions (e.g., Sahu and Saxena 2015; Sahu *et al.* 2016). Being a coastal environment, the land-sea breezes can be an important factor in controlling the CO distribution in the lower troposphere over Chennai, as reported in air-quality studies over several coastal cities, e.g., Athens (Flocas *et al.* 2003), Los Angeles (Lu and Turco 1994), New England (Angevine *et al.* 2004) and Bangkok (Sahu *et al.* 2013b). In most cases, the sea breeze is seen to bring in cleaner oceanic air masses and diluting the concentrations of pollutants over the receptor site. As shown in figure 3, the relationship between CO and wind parameters in the PBL region has been analysed for different seasons. In each wind sector (bin of 45°), the mixing ratio of

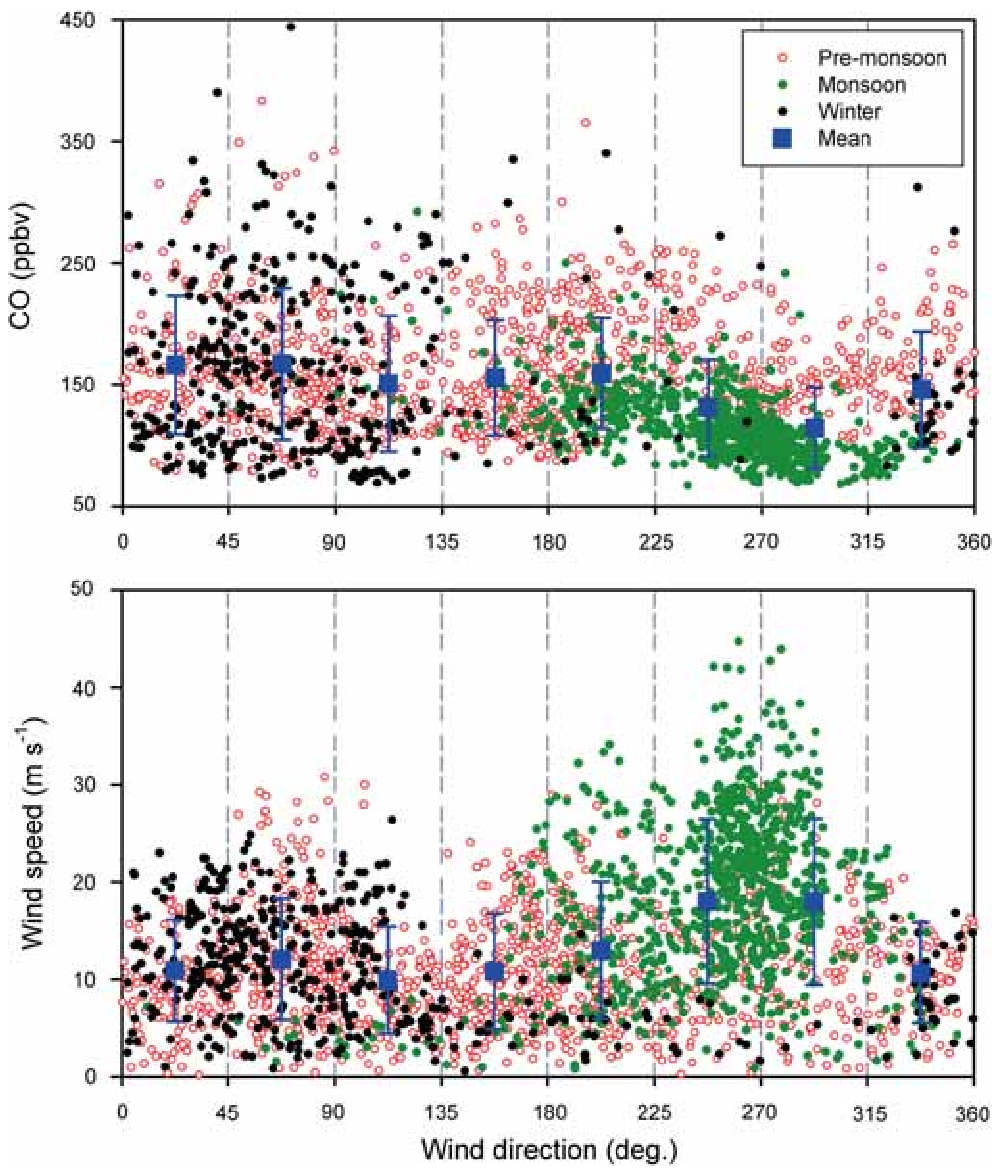

Figure 3. Dependence of the mixing ratios of CO on the wind direction measured in the PBL region for different seasons over Chennai.

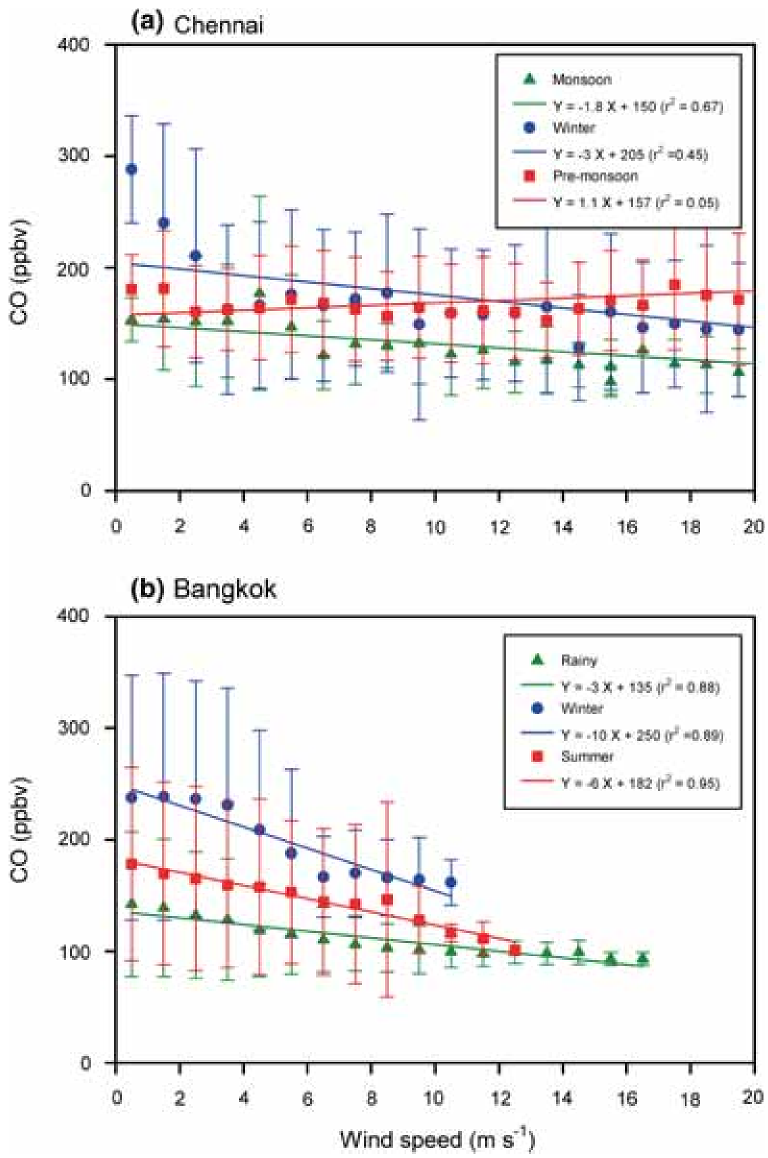

Figure 4. Variation of the CO mixing ratio with wind speed in the lower troposphere over (**a**) Chennai and (**b**) Bangkok. The lines show linear least-squares fit to the data points with the results of the fits given in the legends.

CO and the magnitude of wind speed exhibit large variations. The enhancements of CO in the N–SE (0−135°) sector represent measurements from winter to the pre-monsoon period. In this sector, the average values of CO and wind speed were 165 ppbv and 12 m s^{-1}, respectively. Most of the data points in the SE–SW sector (135−225°) represent pre-monsoon measurements. In this regime, the average values of the CO mixing ratio and wind speed were 155 ppbv and 10 m s^{-1}, respectively. In the SW–NW (225−315°) sector, most of the data represent measurements in the monsoon season. In this sector, the averages of CO and wind speed were 125 ppbv and 18 m s^{-1}, respectively. Clearly, the levels of CO and wind speed demonstrate contrasting tendencies with wind direction in the lower troposphere.

The regression fit of CO (binned at 1.0 m s^{-1}) versus wind speed is shown in figure 4(a). Higher levels of CO (>200 ppbv) during winter were observed under stagnant conditions (1−2 m s^{-1}). CO levels show a gradual decline with the prevalence of stronger winds (>3 m s^{-1}). During the monsoon, CO declined under both low and high wind speed conditions. The declining rates of Δ CO/Δwind speed were estimated to be about −3.0 ppbv/m s^{-1} for winter and −1.8 ppbv/m s^{-1} for the monsoon season. In the winter season, the decline of CO in Chennai was caused by the dilution with cleaner air from the BOB. In the monsoon, the combined effects of lesser biomass burning and cleaner SW winds from the Arabian Sea resulted in the gradual dilution of CO.

Interestingly, the mixing ratio of CO during pre-monsoon exhibits a slight increase with increasing wind speed. For this season, the estimated slope of Δ CO/Δwind speed was positive (1.1 ppbv/m s^{-1}). As shown in the back trajectory plots, the transport of continental air and the lesser influence of maritime air prevailed during the pre-monsoon seasons. Furthermore, the emissions from open biomass fires in India were the most extensive in the pre-monsoon season (Sahu and Sheel 2013a). Therefore, transport and mixing of air with higher backgrounds of CO do not effectively dilute the pollutants under moderate wind speed conditions. However, the enhancements observed under higher winds could be due to the rapid transport from stronger sources located in the upwind regions of Chennai. We have also compared the CO–wind speed relationship at Bangkok (13.8°N, 100.5°E, the nearest MOZAIC airport in the tropics). For this purpose, the MOZAIC data measured in the PBL region over Bangkok for the period 2005–2006 has been analysed (figure 4b). In each season, the levels of CO over Bangkok showed a stronger dependence on wind speed than those observed over Chennai. More detailed observations especially through aircraft-borne instruments are required to further complement this work to quantify the effects of regional-scale transport in relation to those of local origins above Chennai.

3.3 *Dependence of CO on OLR*

Atmospheric conditions are important for the formation and development of the convection system. Strong vertical wind shears inhibit the formation and intensification of deep convection, while deep convection is generally associated with weak

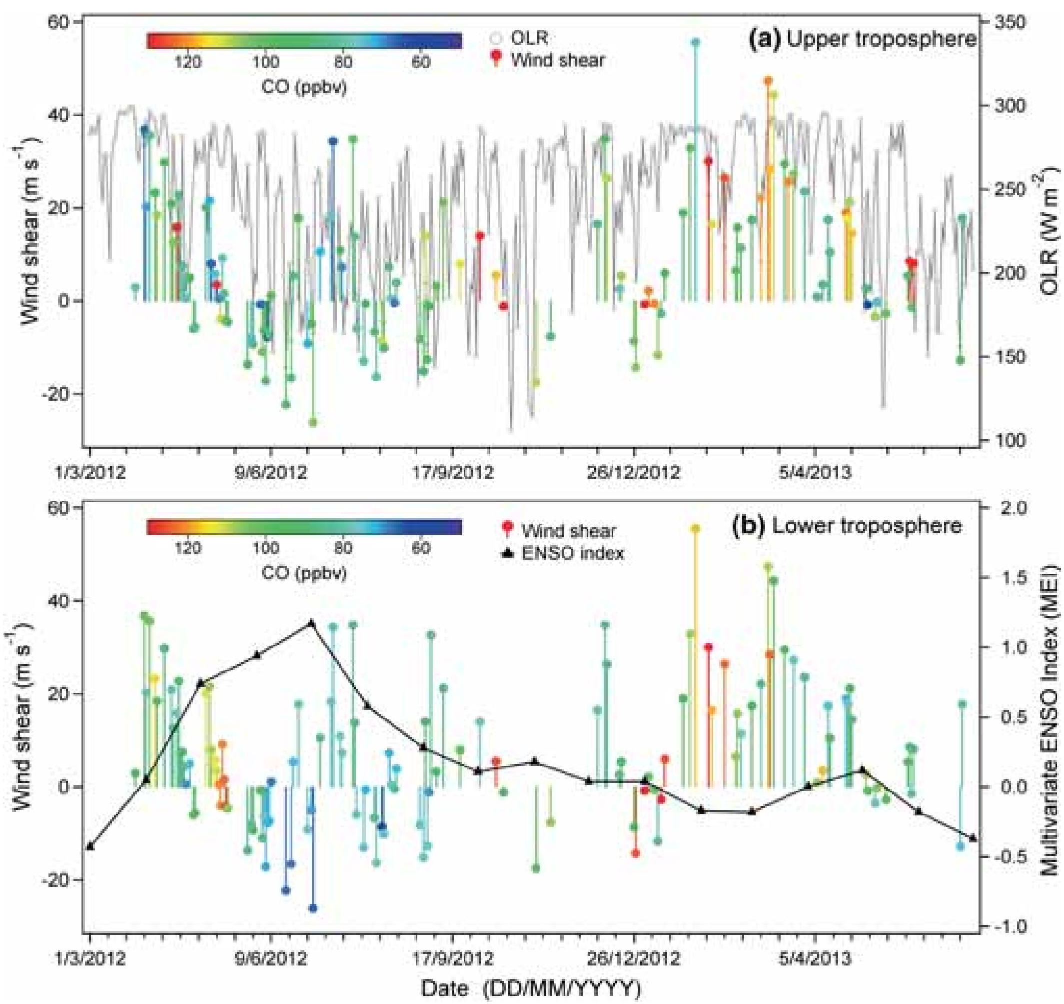

Figure 5. Variations of the MOZAIC flights derived wind shear (average wind speed at 10–12 km – average wind speed at 0–2 km) colour coded with the CO mixing ratio in the upper and lower troposphere over Chennai along with OLR and MEI.

wind shears (Wong and Chan 2004). In the present study, wind shear has been calculated from the MOZAIC wind speed profiles measured during each of the 129 flights over Chennai. The wind shear is the difference of average values of wind speed measured between 0–2 and 10–12 km of altitudes. The main objective of this analysis using wind shear is to understand the role of convection activities in the vertical variations of CO over Chennai. Based on each flight profile data measured during the study period, the time series plots of wind shear data colour-coded with CO measured in the free troposphere are shown in figure 5. The wind shear and OLR data show large flight-to-flight variations and the time series of wind shear tends to follow the pattern of daily OLR over the Chennai region. A higher frequency of strong shears (>10 m s^{-1}) was noticed at the beginning of the pre-monsoon season, while weak/negative shears (<5 m s^{-1}) were observed during the monsoon and post-monsoon seasons. During the El Niño phase between monsoon and post-monsoon 2012, the levels of CO were low in the PBL region and relatively high values were measured in the free troposphere. During this phase, low values of CO in the PBL region and elevated values in the upper troposphere were observed during weak/negative wind shears. During winter–pre-monsoon 2013, under the normal/mild La Niña phase (negative MEI values), elevated values of CO were measured throughout the troposphere. Mostly, the days (or flights) with higher levels of CO coincided with smaller OLR values, implying the influence of deep convection. Therefore, higher values in the upper troposphere during pre-monsoon 2013 than those during the same season in 2012 are attributed to more frequent deep convection activities. On the other hand, the very high mixing ratios of CO (>150 ppbv) in the upper troposphere coincided with high OLR values (>250 W m^{-2}) during some flights in the month of October 2012. The trend of OLR over the South Asia region is influenced by the trend of El Niño-Southern Oscillation (ENSO) conditions which have important implications for the trends of CO mixing ratios in both lower and upper troposphere. In the South Asia region, the El Niño conditions represent the subdued activities of deep convection that lead to the lower vertical transport of CO and higher values of OLR. On the other hand, the development of deep convection is favoured by the La Niña conditions resulting in the efficient vertical transport of CO and lower values of OLR. Therefore, the El Niño phase favours the

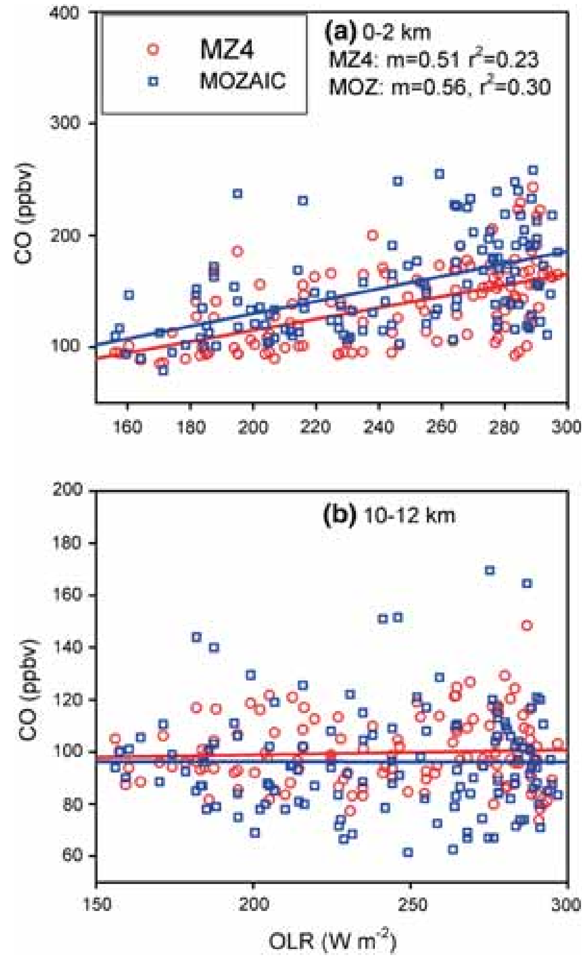

Figure 6. Dependencies of the CO mixing ratios obtained from the MOZAIC observation and MOZART-4 (MZ4) simulation on OLR at 0–2 km (upper panel) and 10–12 km of altitudes (lower panel) over Chennai.

accumulation of CO near the surface and inhibits the transport of CO-rich surface air to the upper troposphere. On the other hand, the La Niña phase favours the ventilation or dispersion of CO near the surface and supports the transport of CO-rich air to the upper troposphere.

The relationship between the CO mixing ratios for both lower and upper troposphere and OLR is presented in figure 6. In the lower troposphere region, the MOZAIC observation and MOZART-4 simulation show a gradual decrease of CO with decreasing OLR. In the lower OLR regimes, particularly, in the monsoon season, the CO–OLR relation suggests the role of the reduced emissions due to the least of activities such as biomass burning and efficient dilution of surface pollutants due to moist convection. In the monsoon season, the emissions of CO from biomass burning sources were minimal in the South Asia region. From winter until early pre-monsoon, the large biomass burning emissions and favourable meteorological conditions lead to higher values of CO and OLR, respectively. The competing effects of higher CO emission in the winter/pre-monsoon season and efficient vertical transport in the monsoon/post-monsoon season reflect the observed relationship between CO and OLR in the upper troposphere. Therefore, the MOZAIC and MOZART-4 simulation of CO in the upper troposphere shows a weaker dependence on OLR.

4. Conclusions

An analysis of aircraft-based in situ measurements of the CO mixing ratio in the troposphere (0–12 km) over Chennai city in India shows significant seasonal variation depending on the altitude. Higher levels of CO in the lower troposphere were observed during the winter season. In the middle and upper troposphere (>6 km), higher levels of CO were measured during the post-monsoon season. In the lower troposphere, values of wind speed measured during the monsoon and post-monsoon seasons were higher compared to those during other seasons. At greater heights, the wind speeds were stronger in winter and weaker during the post-monsoon season. Overall, the mixing ratio profile of CO exhibits a contrasting seasonal tendency to that of the wind speed throughout the troposphere. In the post-monsoon season, as evident from the weaker vertical wind shears, the vertical transport of the CO-rich surface air is favoured by the strong activities of convection over the BOB. The near-surface mixing ratios of CO declined with increasing wind speed, suggesting the major contributions from local sources during the winter and monsoon seasons. The rate of decline (ΔCO/Δwind speed) of -3.0 ppbv/m s^{-1} during the winter season was higher than an estimated value of -1.8 ppbv/m s^{-1} in the monsoon season. The decrease of CO with increasing wind speed in the winter and monsoon seasons were caused by the transport of relatively clean air from the BOB and Arabian Sea, respectively. The relationship between CO and wind parameters in the lower troposphere suggests major enhancements of CO from the winter to the pre-monsoon season due to the prevailing N–SE wind flow. From the winter to the pre-monsoon period of 2013, the elevated mixing ratios of CO coincided with the lower OLR values, indicating the influence of deep convection under the mild La Niña phase. In the lower troposphere, the MOZAIC observation and MOZART-4 simulation exhibit a decrease in CO with decreasing OLR, indicating the role of efficient dilution of CO due to widespread convection activities, mainly during the monsoon and post-monsoon seasons. Meanwhile, in the upper troposphere, the competing effects of higher CO emission during winter to the pre-monsoon period and the rapid vertical updraft of CO-rich moist air during the monsoon/post-monsoon period lead to a weaker dependence of CO on OLR. In summary, persistent and strong enhancements of CO in the free troposphere during the post-monsoon season can be attributed mainly to the widespread activities of convection over peninsular India.

Acknowledgements

The European Commission, Airbus, CNRS-France, FZJ-Germany and the airlines (Lufthansa, Air France, Austrian and former Sabena who have been carrying free of charge, the MOZAIC instrumentation since 1994, are gratefully acknowledged. Our sincere thanks to P Nedelec from Laboratoire d'Aérologie, CNRS, Observatoire Midi-Pyrénées, UMR 5560, 14 Avenue Edouard Belin, 31400 Toulouse, France for encouraging us to use the MOZAIC data for this study. We sincerely thank Dr. M Kajino from the Meteorological Research Institute (MRI), Japan Meteorological Agency (JMA), Tsukuba, for providing us with the back trajectory data.

References

Anenberg S C, West J J, Fiore A M, Jaffe D A, Prather M, Bergmann D, Cuvelier C, Dentener F, Duncan B, Gauss M, Hess P, Jonson J, Lupu A, MacKenzie I, Marmer E, Park R, Sanderson M, Schultz M, Shindell D, Szopa S, Vivanco M G, Wild O and Zeng G 2009 Intercontinenal impacts of ozone pollution on human mortality; *Environ. Sci. Technol.* **43** 6482–6487.

Angevine W M, Senff C J, White A B, Williams E J, Koermer J, Miller S T K, Talbot R, Johnston P E, McKeen S A and Downs T 2004 Coastal boundary layer influence on pollutant transport in New England; *J. Appl. Meteorol.* **43** 1425–1437, https://doi.org/10.1175/JAM2148.1.

Asnani G C 2005 *Tropical Meteorology: Special features of tropical meteorology; Climatology of the tropics; Climatic change; Physics and dynamics of monsoon.* Tropical Meteorology, Volume 1. G.C. Asnani

Emmons L K, Walters S, Hess P G, Lamarque J-F, Pfister G G, Fillmore D, *et al.* 2010 Description and evaluation of the Model for Ozone and Related chemical Tracers, version 4 (MOZART-4); *Geosci. Model Dev.* **3** 43–67, https://doi.org/10.5194/gmd-3-43-2010.

Fishman J and Seiler W 1983 Correlative nature of ozone and carbon monoxide in the troposphere - Implications for the tropospheric ozone budget; *J. Geophys. Res.* **88**, https://doi.org/10.1029/JC088iC06p03662.

Flocas H A, Assimakopoulos V D, Helmis C G and Güsten H 2003 VOC and O_3 distributions over the densely populated area of greater Athens, Greece; *J. Appl. Meteorol.* **42** 1799–1810.

Ghude S D, Beig G, Kulkarni P S, Kanawade V P, Fadnavis S, Remedios J J and Kulkarni S H 2011 Regional CO pollution over the Indian subcontinent and various transport pathways as observed by MOPITT; *Int. J. Remote Sens.* **32**(**21**) 6133–6148.

Girach I A and Nair P R 2014 Carbon monoxide over Indian region as observed by MOPITT; *Atmos. Environ.* **99** 599–609.

Girishkumar M S and Ravichandran M 2012 The influences of ENSO on tropical cyclone activity in the Bay of Bengal during October–December; *J. Geophys. Res.* **117** C02033, https://doi.org/10.1029/2011JC007417.

Granier C, Lamarque J F, Mieville A, Muller J F, Olivier J, Orlando J, Peters J, Petron G, Tyndall G and Wallens S 2005 POET, a database of surface emissions of ozone precursors; http://www.aero.jussieu.fr/projet/ACCENT/POET.php.

Jöckel P, Tost H, Pozzer A, Kunze M, Kirner O, Brenninkmeijer C A M, Brinkop S, Cai D S, Dyroff C, Eckstein J, Frank F, Garny H, Gottschaldt K-D, Graf P, Grewe V, Kerkweg A, Kern B, Matthes S, Mertens M, Meul S, Neumaier M, Nützel M, Oberländer-Hayn S, Ruhnke R, Runde T, Sander R, Scharffe D and Zahn A 2016 Earth system chemistry integrated modelling (ESCiMo) with the modular earth submodel system (MESSy) version 2.51; *Geosci. Model Dev.* **9** 1153–1200, https://doi.org/10.5194/gmd-9-1153-2016.

Kar J, Jones D B A, Drummond J R, Attie J L, Liu J, Zou J, Nichitiu F, Seymour M D, Edwards D P, Deeter M N, Gille J C and Richter A 2008 Measurement of low altitude CO over the Indian subcontinent by MOPITT; *J. Geophys. Res. Atmos.* **113** D16307.

Lelieveld J, Bourtsoukidis E, Brühl C, Fischer H, Fuchs H, Harder H, Hofzumahaus A, Holland F, Marno D, Neumaier M, Pozzer A, Schlager H, Williams J, Zahn A and Ziereis H 2018 The South Asian monsoon-pollution pump and purifier; *Science*, https://doi.org/10.1126/science.aar2501.

Lu R and Turco R P 1994 Air pollutant transport in a coastal environment.1. 2-dimensional simulations of sea-breeze and mountain effects; *J. Atmos. Sci.* **51** 2285–2308.

Nedelec P, *et al.* 2003 An improved infrared carbon monoxide analyser for routine measurements aboard commercial Airbus aircraft: Technical validation and first scientific results of the MOZAIC III programme; *Atmos. Chem. Phys.* **3** 1551–1564, https://doi.org/10.5194/acp-3-1551-2003.

Ohara T, Akimoto H, Kurokawa J, Horii N, Yamaji K, Yan X and Hayasaka T 2007 An Asian emission inventory of anthropogenic emission sources for the period 1980–2020; *Atmos. Chem. Phys.* **7** 4419–4444, https://doi.org/10.5194/acp-7-4419-2007.

Ojha N, Pozzer A, Rauthe-Schöch A, Baker A K, Yoon J, Brenninkmeijer C A M and Lelieveld J 2016 Ozone and carbon monoxide over India during the summer monsoon: Regional emissions and transport; *Atmos. Chem. Phys.* **16** 3013–3032.

Prockop L D and Chichkova R I 2007 Carbon monoxide intoxication: An updated review; *J. Neurol. Sci.* **262** 122–130.

Randel W, Park M, Emmons L, Kinnison D, Bernath P, Walker K, Boone C and Pumphrey H 2010 Asian monsoon transport of pollution to the stratosphere; *Science* **328** 611, https://doi.org/10.1126/science.1182274.

Rauthe-Schöch A, Baker A K, Schuck T J, Brenninkmeijer C A M, Zahn A, Hermann M, Stratmann G, Ziereis H, van Velthoven P F J and Lelieveld J 2016 Trapping, chemistry, and export of trace gases in the South Asian summer monsoon observed during CARIBIC flights in 2008; *Atmos. Chem. Phys.* **16** 3609–3629, https://doi.org/10.5194/acp-16-3609-2016.

Sahu L K and Sheel V 2013 Spatio-temporal variation of biomass burning sources over South and Southeast Asia; *J. Atmos. Chem.* **71** 1–19, https://doi.org/10.1007/s10874-013-9275-4.

Sahu L K and Saxena P 2015 High time and mass resolved PTR-TOF-MS measurements of VOCs at an urban site of India during winter: Role of anthropogenic, biomass burning, biogenic and photochemical sources; *Atmos. Res.* **164–165** 84–94.

Sahu L K, Lal S, Thouret V and Smit H G 2011 Climatology of tropospheric ozone and water vapour over Chennai: A study based on MOZAIC measurements over India; *Int. J. Climatol.* **31** 920–936, https://doi.org/10.1002/joc.2128.

Sahu L K, Sheel V, Kajino M and Nedelec P 2013 Variability in tropospheric carbon monoxide over an urban site in Southeast Asia; *Atmos. Environ.* **68** 243–255.

Sahu L K, Yadav R and Pal D 2016 Source identification of VOCs at an urban site of western India: Effect of marathon events and anthropogenic emissions; *J. Geophys. Res. Atmos.* **121** 1–18.

Sahu L K, Tripathi N, Sheel V, Kajino M, Deushi M, Yadav R and Nedelec P 2018 Impact of the tropical cyclone 'Nilam' on the vertical distribution of carbon monoxide over Chennai on the Indian peninsula; *Quart. J. Roy. Meteorol. Soc.*, https://doi.org/10.1002/qj.3276.

Sheel V, Sahu L K, Kajino M, Deushi M, Stein O and Nedelec P 2014 Seasonal and interannual variability of carbon monoxide based on MOZAIC observations, MACC reanalysis, and model simulations over an urban site in India; *J. Geophys. Res. Atmos.* **119** 9123–9141, https://doi.org/10.1002/2013JD021425.

Sheel V, Bisht J H, Sahu L and Thouret V 2016 Spatio-temporal variability of CO and O3 over a site in central India based on MOZAIC observations and WRF/Chem and MOZART-4 models; *Tellus B* **68** 30545, https://doi.org/10.3402/tellusb.v68.30545.

Shindell D T, Faluvegi G, Stevenson D S, Krol M C, Emmons L K, Lamarque J-F, Pétron G, Dentener F J, Ellingsen K, Schultz M G, Wild O, Amann M, Atherton C S, Bergmann D J, Bey I, Butler T, Cofala J, Collins W J, Derwent R G, Doherty R M, Drevet J, Eskes H J, Fiore A M, Gauss M, Hauglustaine D A, Horowitz L W, Isaksen I S A, Lawrence M G, Montanaro V, Müller J-F, Pitari G, Prather M J, Pyle J A, Rast S, Rodriguez J M, Sanderson M G, Savage N H, Strahan S E, Sudo K, Szopa S, Unger N, vanNoije T P C and Zeng G 2006 Multimodel simulations of carbon monoxide : Comparison with observations and projected near-future changes; *J. Geophys. Res.* **111** D19306, https://doi.org/10.1029/2006JD007100.

Stohl A, Eckhardt S, Forster C, James P and Spichtinger N 2002 On the pathways and timescales of intercontinental air pollution transport; *J. Geophys. Res.* **107** 4684, https://doi.org/10.1029/2001JD001396.

Ueno K and Aryal R 2007 Impact of tropical convective activity on monthly temperature variability during nonmonsoon season in the Nepal Himalayas; *J. Geophys. Res.* **113** D18112, https://doi.org/10.1029/2007JD0095242008.

Wong M L and Chan J C 2004 Tropical cyclone intensity in vertical wind shear; *J. Atmos. Sci.* **61(15)** 1859–1876, https://doi.org/10.1175/1520-0469(2004)061<1859:TCIIVW>2.0.CO;2.

Worden J, Wecht K, Frankenberg C, Alvarado M, Bowman K, Kort E, Kulawik S, Lee M, Payne V and Worden H 2013 CH_4 and CO distributions over tropical fires during October 2006 as observed by the Aura TES satellite instrument and modeled by GEOS-Chem; *Atmos.Chem. Phys.* **13(7)** 3679–3692, https://doi.org/10.5194/acp-13-3679-2013.

Yadav R, Sahu L K, Jaaffrey S N A and Beig G 2014 Distribution of ozone and related trace gases at an urban site in western India; *J. Atmos. Chem.* **71** 125–144.

Yoon J and Pozzer A 2014 Model-simulated trend of surface carbon monoxide for the 2001–2010 decade; *Atmos. Chem. Phys.* **14** 10465–10482, https://doi.org/10.5194/acp-14-10465-2014.

Zhang L, *et al.* 2011 Impacts of 2006 Indonesian fires and dynamics on tropical upper tropospheric carbon monoxide and ozone; *Atmos. Chem. Phys.* **11** 10929–10946, https://doi.org/10.5194/acp-11-10929-2011.

Corresponding editor: Suresh Babu